Nonsense *CD247* mutations show dominant-negative features in T-cell receptor expression and function

Alejandro C. Briones, PhD, Rebeca F. Megino, MSc, Ana V. Marin, PhD, Daniel Chacón-Arguedas, MSc, Elena García-Martinez, MSc, Héctor Balastegui-Martín, MD, et al

GRAPHICAL ABSTRACT

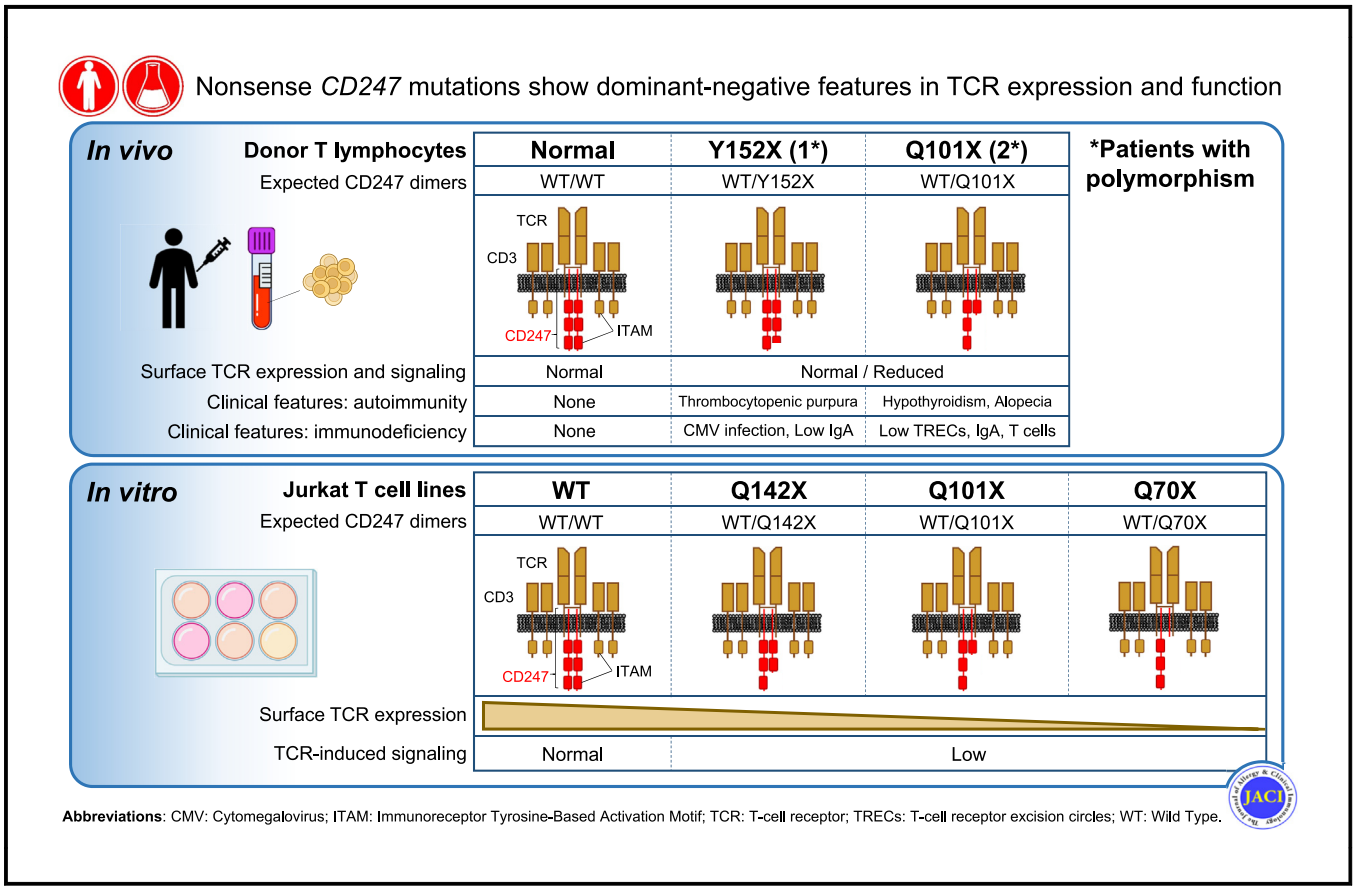

Capsule summary: CD247 variants without ITAMs exhibited a dominant-negative effect on normal TCR expression and signaling *in vitro.* This may contribute to immune dysregulation *in vivo,* as seen in 3 carrier patients.

J Allergy Clin Immunol 2024;■■■:■■■-■■■.

https://doi.org/10.1016/j.jaci.2024.06.019

Nonsense *CD247* mutations show dominant-negative features in T-cell receptor expression and function

Alejandro C. Briones, PhD,[a]* Rebeca F. Megino, MSc,[a]* Ana V. Marin, PhD,[a] Daniel Chacón-Arguedas, MSc,[a] Elena García-Martinez, MSc,[b] Héctor Balastegui-Martín, MD,[b] Hugh T. Reyburn, PhD,[c] Sarah E. Henrickson, MD, PhD,[d,e] Carmen Rodríguez-Sainz, PhD,[b] Elena Seoane-Reula, MD, PhD,[f] Paloma Sanchez-Mateos, MD, PhD,[b] Paula P. Cardenas, PhD,[a]* and Jose R. Regueiro, PhD[a]*

Madrid, Spain; and Philadelphia, Pa

Background: The invariant TCR ζ/CD247 homodimer is crucial for TCR/CD3 expression and signaling through its 3 immunoreceptor tyrosine-based activation motifs (ITAMs). Homozygous null mutations in *CD247* lead to immunodeficiency, while carriers exhibit 50% reduced surface CD3. It is unclear whether carriers of other *CD247* variants show dominant-negative effects.

Objective: We sought to analyze and model the potential impact on T-cell receptor (TCR) expression and function of heterozygous nonsense *CD247* mutations found in patients with signs of immunodeficiency or autoimmunity.

Methods: Jurkat T cells, either wild-type (WT) or CRISPR/Cas9-edited CD247-deficient (ZKO), were lentivirally transduced with WT CD247 or mutations ablating 1 (Q142X), 2 (Q101X), or 3 (Q70X) ITAMs.

Results: Three patients from unrelated families were studied. Two heterozygous nonsense *CD247* mutations were identified (p.Y152X and p.Q101X), which affected ITAM-3 and ITAM-2 and ITAM-3, respectively. Both mutations were associated with low surface CD3 expression and normal intracellular CD247 levels using a transmembrane-specific antibody, but very low intracellular CD247 levels using an ITAM-3–specific one, suggesting the presence of truncated variants in T cells. Transduction of the mutations lacking 1, 2, or 3 ITAMs into ZKO cells could not restore normal surface CD3 expression (only 60%, 22%, and 10%, respectively), whereas in WT cells, normal surface CD3 expression was reduced (to 39%, 19%, and 9% of normal levels), and both effects were dependent on ITAM number. All 6 transfectants showed reduced CD69 induction (25% to 50%), indicating that they were unable to signal downstream properly, neither isolated nor associated with WT CD247.

Conclusions: Our results suggest that *CD247* variants lacking ITAMs due to nonsense, but not null, mutations are defective for normal TCR assembly and exert a dominant-negative effect on TCR expression and signaling *in vitro*. This, in turn, may correlate with clinical features *in vivo*. (J Allergy Clin Immunol 2024;■■■:■■■-■■■.)

Key words: *CD247, TCR ζ, CD3ζ, TCR, ITAM, immunodeficiency, autoimmunity*

Abbreviations used

crRNA:	CRISPR RNA
iCD247:	Intracellular CD247
ITAM:	Immunoreceptor tyrosine-based activation motifs
NK:	Natural killer
PHA-L:	Phytohemagglutinin-L
SCID:	Severe combined immunodeficiency
SEE:	Staphylococcal enterotoxin E
tracrRNA:	Trans-activating CRISPR RNA
TCR:	T-cell receptor
TEMRA:	Terminal effector memory T cells
WT:	Wild-type

The T-cell receptor (TCR) is a T-cell lineage-specific ensemble involved in antigen recognition. Its stimulation triggers critical responses such as activation, proliferation, differentiation, and anergy or apoptosis at different points of T-cell development.[1] The TCR is a tetradimeric complex made up of a clonotypic heterodimer (TCR αβ or γδ), which binds antigens, and 3 invariant dimers, the CD3δε and CD3γε heterodimers and the CD247 homodimer (also named TCR ζ or CD3ζ),[2] which participate in the assembly and surface expression of the TCR as well as in the transmission of intracellular signals to downstream pathways. Natural killer (NK) cells also express CD247 chains, which signal for several cell surface receptors, including CD16. The CD247 chain is formed by a very short extracellular portion, a transmembrane region involved in dimerization and interaction with other TCR receptor chains, and a long intracellular region with 3 immunoreceptor tyrosine-based activation motifs (ITAMs) domains. CD247 ITAMs have attracted great interest in recent years because they are critical for chimeric antigen receptor T-cell function, although it is still

From [a]the Department of Immunology, Ophthalmology and ENT, Complutense University School of Medicine and 12 de Octubre Health Research Institute (imas12), Madrid; [b]the Department of Immunology, Hospital General Universitario Gregorio Marañón, Madrid; [c]the Department of Immunology and Oncology, National Centre for Biotechnology, Spanish National Research Council (CNB-CSIC), Madrid; [d]the Division of Allergy and Immunology, Department of Pediatrics, Children's Hospital of Philadelphia, University of Pennsylvania, Philadelphia; [e]the Department of Microbiology and Institute of Immunology and Immune Health, Perelman School of Medicine, University of Pennsylvania, Philadelphia; and [f]Pediatric Immunodeficiency Unit, Hospital General Universitario Gregorio Marañón, Madrid.

*These authors contributed equally to this work.

Received for publication January 4, 2024; revised May 31, 2024; accepted for publication June 18, 2024.

Corresponding author: Jose R. Regueiro, PhD, Department of Immunology, Ophthalmology and ENT, School of Medicine, Complutense University, 28040 Madrid, Spain. E-mail: regueiro@ucm.es.

0091-6749

https://doi.org/10.1016/j.jaci.2024.06.019

controversial whether more or less or which ITAMs are required for exhaustion versus improved immunotherapy.[3-5]

CD247 is crucial for normal TCR expression and signaling.[6] Homozygous null mutations in humans cause severe combined immunodeficiency (SCID), characterized by a severe reduction of surface TCR levels associated with T-cell lymphopenia and recurrent infections.[7] Carriers of null mutations show no clinical features despite decreased surface TCR (50% vs normal). It is unclear if carriers of non-null *CD247* variants may show dominant-negative effects in TCR expression or function.

We studied 3 patients from unrelated families showing signs of immunodeficiency or autoimmunity and carrying nonsense heterozygous *CD247* mutations (p.Y152X and p.Q101X), which affected 1 or 2 ITAMs, respectively. Here, we analyzed the impact of different ITAM-ablating *CD247* mutations in TCR expression and function both *ex vivo* and *in vitro* using CD247-sufficient (wild-type [WT]) and CD247-deficient (ZKO) Jurkat T cells as a model system. The results support the existence of dominant-negative effects, which may be associated with immune pathology.

METHODS

Immunophenotype

Purification and isolation of PBMCs were performed by gradient centrifugation on Ficoll-Paque PLUS (Cytiva, Marlborough Mass). PBMC populations were analyzed by extracellular flow cytometry with mAbs against CD3 (clones UCHT-1, S4.1, SK7, and HIT3A) from BD Biosciences (Franklin Lakes, NJ) or BioLegend (San Diego, Calif), CD4 (13B8.2 or RPA-74) and CD31 from BD Biosciences, CD56 (NCAM-1) from Beckman Coulter (Brea, Calif), TCR αβ (IP26) from Thermo Fisher Scientific (Waltham, Mass), γδTCR (11F2) and CCR7 from BioLegend, CD45RA from eBioscience (San Diego, Calif), and CD45RO from Immunotech (Beckman Coulter Immunotech, Marseille, France) or by intracellular flow cytometry using mAbs against CD247 (clones 6B10.2 from BioLegend and H146-968 from Sigma-Aldrich [St Louis, Mo]). Intracellular staining was done with the FOXP3/Transcription factor staining buffer set (Invitrogen, Waltham, Mass). Data were acquired with a FACSCalibur or FACSCelesta flow cytometer (BD Biosciences) and analyzed with FlowJo software (TreeStar, Ashland, Ore).

Cell lines

Jurkat T cells (J77cl20 clone) were grown in RPMI-1640 without L-glutamine media (Lonza, Basel, Switzerland) supplemented with 10% FBS, 1× L-glutamine 200 mM, and 1× Antibiotic-Antimycotic from Gibco Life Technologies (Bethesda, Md). The HEK293T packaging cell line was grown under standard conditions in Iscove Modified Dulbecco Medium (Lonza, Basel, Switzerland). All cell lines were maintained at 37°C and 5% CO_2 in a humidified incubator.

CD247-deficient Jurkat T cells

CD247-specific CRISPR RNA (crRNA) (5′-GCTCAATCTAGGACGAAGAGAGG-3′) and trans-activating CRISPR RNA (tracrRNA) (5′-AGCAUAGCAAGUUAAAAUAAGGCUAGUCCGUUAUCAACUUGAAAAAGUGGCACCGAGUCGGUGCUUU-3′) were designed and synthesized by Integrated DNA Technologies (Coralville, Iowa). To form the crRNA:tracrRNA complex, 2.2 μL of 200-μM crRNA and 2.2 μL of 200-μM tracrRNA were mixed and heated at 95°C for 5 minutes. The mixture was then incubated at room temperature for 30 minutes. Ribonucleoprotein complexes were prepared by incubating 18 μM Cas9 with 22 μM crRNA:tracrRNA duplex in Resuspension Buffer R from Neon System kit (Invitrogen) at room temperature for 20 minutes.

Jurkat T cells were electroporated with a Neon transfection kit and device (Invitrogen). Briefly, 0.5×10^5 T cells resuspended in Buffer R from the Neon kit were mixed with 3 μM Cas9 ribonucleoprotein in a final volume of 11 μL. Using a Neon electroporation device (1600 V, 10 ms, 3 pulses), 10 μL of the suspension were electroporated. Electroporated cells were resuspended in prewarmed culture medium and incubated for 72 hours. Cell sorting was then performed to isolate the $CD3^-$ population, followed by limiting dilution to obtain single-cell clones.

For genetic analysis of purified clones, genomic DNA was extracted by QuickExtract DNA Extraction Solution (Epicentre Biotechnologies, Madison, Wis) and amplified using a pair of primers containing the targeted site with Phusion High-Fidelity DNA Polymerase (New England Biolabs, Ipswich, Mass). The PCR products were purified using QIAquick PCR Purification Kit (QIAGEN, Hilden, Germany) followed by Sanger sequencing. The sequencing data were analyzed using TIDE online software (https://tide.nki.nl).

Plasmids and lentiviral transduction

For lentiviral transduction, *CD247* WT/Iso-2 or Iso-1 splicing variants of normal *CD247* as well as *CD247* variants ablating 1 (Q142X), 2 (Q101X), or 3 (Q70X) ITAMs were introduced in pHRSIN-C56W-UbEM lentiviral plasmid, and HEK293T cells were transfected with Lipofectamine 2000 (Invitrogen), together with the plasmids psPAX2 and pMD2G. Two days after transfection, culture media containing the viral particles was harvested, filtered, and stored at −80°C. For each transduction, 0.1×10^6 cells were incubated in 0.75 mL of viral supernatant with 6 μM BX795 (InvivoGen, San Diego, Calif) and 8 μg/mL Polybrene (Sigma-Aldrich, Burlington, Mass) seeded in a U-Bottom 96-well plate (BD Biosciences). The plates were centrifuged at 800 rpm and 33°C for 1 hour. After centrifugation, the plates were incubated for 4 to 6 hours at 37°C in a 5% CO_2 atmosphere without removing viral supernatants and later centrifuged in the same conditions. Supernatants were removed from wells, and fresh medium was added.

The pEGFP-N1 vector (Clontech Laboratories, Mountain View, Calif) containing the CD247 transcript variant or isoform 2 sequence (NM_000734; henceforth CD247 Iso-2/WT) or the germline p.Q70X mutation was used. The CD247 transcript variant or isoform 1 (NM_198053; henceforth CD247 Iso-1) and germline mutations p.Q101X (Variation ID: 419227) and p.Q142X (Variation ID: 466358) were introduced by site-directed mutagenesis and restriction cloning.

Functional studies

A total of 0.2×10^6 PBMCs were incubated in flat-bottom 96-well plates with RPMI-1640 supplemented with 10% FBS in the presence or absence of Dynabeads T-Activator CD3/CD28 (Thermo Fisher Scientific) and analyzed with anti-CD69 (L-78)

and anti-CD25 (CD25-3G10) by flow cytometry after 24 and 48 hours, respectively. Proliferation was measured by dilution of the cell tracer carboxyfluorescein diacetate succinimidyl ester (Thermo Fisher Scientific). Briefly, cells were stained with 5 μM carboxyfluorescein diacetate succinimidyl ester and stimulated with 1 μg/mL UCHT-1 (BioLegend) or 5 μg/mL phytohemagglutinin-L (PHA-L) from *Phaseolus vulgaris* (Sigma-Aldrich) for 5 days. Cells were then collected and stained with anti-CD4 (Beckman Coulter) and anti-CD8 (BioLegend) to determine the proliferation index (total number of cell divisions divided by cells that went into division) in these populations separately.

For conjugation assays, WT or ZKO Jurkat T-cell lines expressing different CD247 variants were cocultured with antigen-presenting Raji cells (ratio 1:1) preloaded with 0.5 μg/mL staphylococcal enterotoxin E (SEE) (Sigma-Aldrich) for 18 hours in round-bottom 96-well plates. Next, cells were collected and stained with anti-CD69 to evaluate TCR-induced function and anti-CD19 (HIB19; BD Biosciences) to discriminate Jurkat cells from Raji cells. We tried to conduct conjugate experiments in primary T cells, but the proportion of conjugates was too small to reach meaningful conclusions, as the primary T-cell population was in all cases polyclonal (in contrast to Jurkat cells, which are monoclonal) and in many cases scarce.

Fluorescence microscopy

For fluorescence microscopy studies, 1.5×10^6 ZKO Jurkat cells were electroporated with 2 μg of pEGFP-N1 plasmid, carrying each *CD247* variant, using the Cell Line Optimization Nucleofector Kit V and the Amaxa Nucleofector Transfection 2b device (both from Lonza, Walkersville, Md), according to the manufacturer's instructions. After 20 hours of transfection, the cells were harvested and washed with 1× PBS. Then, cells were permeabilized with 4% paraformaldehyde during 10 minutes, followed by centrifugation and washing with 1× PBS. Finally, the cells were spread onto a microscope slide, dried, and mounted in ProLong Diamond Antifade Mountant Media with 4′-6-diamidino-2-phenylindole (Life Technologies, Eugene, Ore).

Three-dimensional structure and folding free energy predictions

Protein structure predictions were generated for the variants studied in CD247. The leader peptide amino acid sequences were removed, and only the extracellular, transmembrane and cytoplasmic regions were analyzed using AlphaFold[8,9] through the Phenix suite of crystallography software graphical interface, GUI.[10] After obtaining the 3-dimensional (3D) models, the ScooP algorithm[11] was used to predict the folding free energy $\Delta G(T)$ (http://babylone.ulb.ac.be/SCooP).

Statistical analysis

Patient grouped results are represented as scatter dot plots compared with the normal 5th, 50th, and 95th percentiles in boxes. Using GraphPad Prism 9 (GraphPad Software, Boston, Mass), 2-way ANOVA with Tukey multiple comparison test was applied to data sets. *P* values less than .05 were considered significant.

Patients

Written informed consent to participate in this study was provided by the participants or participants' legal guardian/next of kin. See Fig 1, *A,* and Table I.[12-15]

Family A. A 6-week-old male infant with no previous family history of immunological diseases underwent a neonatal screening for SCID, yielding 5.269 per 10^6 $CD3^+$ T cells (normal yield is > 6.794). The infant was small for gestational age with low-degree macrocephaly. The hemogram showed moderate neutropenia and T-cell lymphopenia. The SCID genetic panel revealed a heterozygous variant (c.301C>T, p.Q101X) in the *CD247* minor Iso-1 splicing isoform. He was managed with *Pneumocystis jirovecii* pneumonia prophylaxis using sulfamethoxazole-trimethoprim (Bactrim, Mutual Pharmaceutical Company, Philadelphia, Pa) and follow-up lymphocyte counts, which have been declining over time due to T-cell loss (Table I). Response to pokeweed mitogen and PHA-L was normal, whereas immunoglobulin levels were low despite showing high numbers of B cells. The patient has remained fit and infection-free.

Family B. A 50-year-old woman presented with episodes of alopecia areata and autoimmune hypothyroidism compatible with a polyglandular syndrome. She had a family history of thyroiditis, and laboratory analysis revealed the presence of anti-thyroid antibodies and a moderate increase in $CD4^+$ T lymphocytes, particularly of terminal effector memory T cells (TEMRA) and $CD45R0^+$ subsets. Biochemistry and blood counts were normal, including B cells and immunoglobulins. A genetic study found the p.Q101X variant in heterozygosity. The genetic study of the family revealed an asymptomatic brother with the same variant and increased TEMRA $CD4^+$ T cells. Mitogen responses to PHA-L and anti-CD3 were high and normal, respectively.

Family C. An 8-year-old girl presented with chronic immune thrombocytopenic purpura since age 3, initially associated with primary cytomegalovirus infection and refractory to several lines of treatment (currently receiving mycophenolate). Mitogen responses to PHA-L and anti-CD3 were normal and low, respectively. Genetic analysis by next-generation sequencing of a panel of 200 immunodeficiency genes identified only a heterozygous c.456C>A mutation in the *CD247* gene. This mutation generates a premature stop codon in the middle of the third ITAM domain (p.Y152X). The genetic study of the family found her mother and her sister were asymptomatic carriers. The mother was positive for rheumatoid factor and had low C3 and C4 levels, as well as slightly increased $CD45R0^+$ $CD4^+$ T cells. The sister shared with the patient reduced NK cell numbers (Table I).

RESULTS

Primary T lymphocytes carrying heterozygous nonsense CD247 variants p.Y152X or p.Q101X showed T- and NK-specific TCR and/or CD247 expression defects

We analyzed extracellular (TCR αβ and CD3) (Fig 2; Fig E1 in this article's Online Repository at www.jacionline.org) and intracellular (CD247) (Fig 3; Fig E2 in the Online Repository available at www.jacionline.org) TCR/CD3 complex epitopes expression in primary lymphocytes from patients and healthy carriers compared with noncarriers and healthy donors using different mAbs that recognize distinct TCR, CD3, or CD247

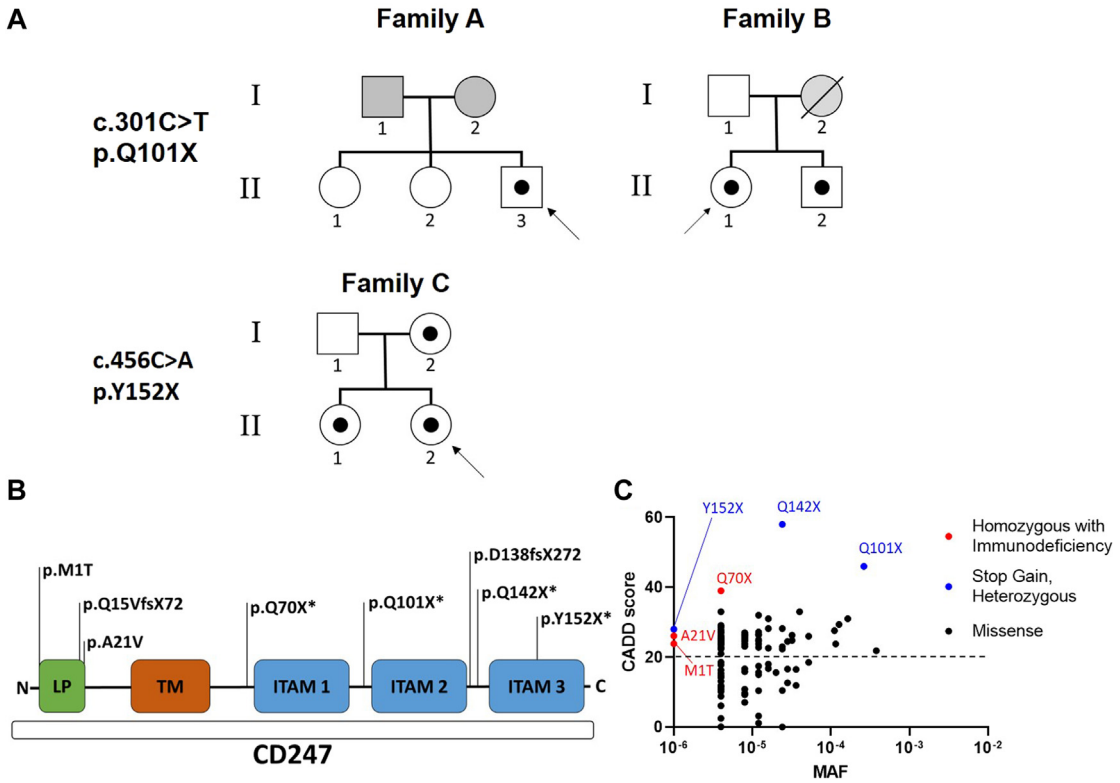

FIG 1. Heterozygous *CD247* mutations in 3 families. **(A)** Pedigree of studied individuals. *Gray* indicates unavailable pedigree; *arrows* point to index cases. **(B)** Schematic representation of the human *CD247* gene with all published or ClinVar-reported mutations indicated. *Asterisks* indicate variants studied in this work. **(C)** Combined annotation-dependent depletion score and the minor allele frequency for all CD247 variants reported in the PopViz database.[12] Combined annotation-dependent depletion scores above 20 *(horizontal broken line)* are considered high. *CADD,* Combined annotation-dependent depletion; *LP,* leader peptide; *MAF,* minor allele frequency; *TM,* transmembrane.

epitopes. This epitope scanning technique provides a rich evaluation of TCR conformational aspects, as reported previously for congenital CD3 immunodeficiencies.[7]

The analysis of extracellular TCR epitopes showed that both CD247 variants were associated with low surface TCR αβ and CD3 expression in T lymphocytes. This was especially evident with certain mAb clones and T-cell types (eg, HIT3A in $CD8^+$ T cells) (Fig E1, right panel), suggesting subtle conformational defects in their TCR. The staining discrepancies between the mutations and the different antibodies used for staining likely reveal the different contribution of the mutant CD247 proteins to the final conformation of the surface TCR for some, but not all, mAbs.

Intracellular CD247 (iCD247) staining was performed using 2 mAbs, 6B10.2 and H146-968 clones, which recognize transmembrane and ITAM-3 epitopes, respectively. The results in patient AII.3 showed that T and NK lymphocytes carrying the CD247 variant p.Q101X were associated with low levels of iCD247 using 6B10.2 and very low intracellular WT CD247 using H146-968 (Fig 3, *A* and *B*, bottom panel). This supports the expression of the truncated variant in such lymphocytes, since 6B10.2 detects both WT and truncated CD247 proteins, whereas H146-968 detects only WT CD247 (Fig 3, *B*, top panel). However, those expression defects were strongly reduced when the T cells were cultured *in vitro* for 2 weeks with allogeneic stimuli (Fig 3, *C*). Indeed, normal iCD247 levels were observed using both mAbs in the 2 carriers from family B (Fig 3, *B*, bottom panel), indicating that the truncated variant was not present in day 15 cultured T cells from AII.3 or in primary T cells from BII.1 or BII.2 (tested when adults). In contrast, T lymphocytes carrying CD247 variant p.Y152X were associated with normal iCD247 using 6B10.2 and very low WT iCD247 using H146-968 in the 3 carriers from family C (Fig 3, *B*, bottom panel), again suggesting expression of the truncated variant in such lymphocytes. Comparable results were found in $CD8^+$ and NK lymphocytes (Fig E2).

Taken together, these results suggested that the truncated variants were expressed in T cells of some of the tested individuals and caused biochemical defects detectable only using CD247-specific mAbs, associated with surface TCR defects detectable using certain TCR αβ– or CD3-specific mAb in T cells.

The contrasting results observed for iCD247 expression in lymphocytes from carriers of the p.Q101X variant, depending on donor age *ex vivo* versus TCR stimulation *in vitro*, begged an explanation. Indeed, variant p.Q101X is peculiar because it occurs only in the minor *CD247* long splicing Iso-1 transcript (20% to 50% of all transcripts),[16] whose biological role and regulation are yet unclear. It has been reported to increase its expression after TCR engagement and to signal poorly compared with WT. In contrast, the main *CD247* short-splicing WT transcript lacks the Q101

TABLE I. Comparative clinical and immunologic features of *CD247* mutation carriers

	Family						
	A		B		C		
Subject	**II.3***		**II.1***	**II.2**	**I.1**	**II.1**	**II.2***
Age at diagnosis	6 wk	6 mo	50 y	48 y	44 y	14 y	8 y
Immunodeficiency	Low TRECs		No	No	No	No	CMV
Autoimmunity	No		AA, TgAb, AH	No	RF (342 U/mL)	No	ITP
Mutation	p.Q101X		p.Q101X			p.Y152X	
PBLs (cells/μL)	3.338†	2.510†	3.000	1.900	1.800	1.900	2.100†
B cells	1.393‡	1.593‡	283	380	313	418	330
NK cells	806	141	481	388	190	68†	49†
T cells ($CD3^+$)	1.132†	712†	2.459‡	1.159	1.143	1.337	1.667
$CD4^+$	813†	513†	1.640‡	881	709	923	1.086
$CD8^+$	303†	185†	775	243	390	351	529
CD4 cell maturation							
$CD45RA^+$	—	387	290	124	240	490	718
RTE ($CD31^+$)	—	342	223	61	168	431	678
TEMRA ($CCR7^-$)	—		170‡	96‡	41	33	11
$CD45RO^+$	—	104	439‡	212	510‡	250	304
Immunoglobulins (mg/dL)							
IgG (660-1620)	—	127†	866		1.150		841
IgA (81-446)	—	<13†	215		244		39†
IgM (49-302)	—	26†	110		162		59
Mitogen responses							
PHA-L	Normal	Normal	High‡	High‡	Normal	Normal	Normal
Anti-CD3	—	—	Normal	Normal	Normal	Normal	Low†

Mitogen responses are quantified in Fig E4 (in the Online Repository available at www.jacionline.org).

AA, Alopecia areata; *AH,* autoimmune hypothyroidism; *CMV,* cytomegalovirus; *ITP,* immune thrombocytopenic purpura; *RF,* rheumatic factor (normal <20 U/mL); *RTE,* recent thymic emigrants; *TgAb,* anti-thyroglobulin antibodies; *TRECs,* T-cell receptor excision circles.

*Index cases.

†Value below normal range for subject's age.[13-15]

‡Value above normal range for subject's age.[13-15]

residue codon and thus cannot have such mutation (Fig 3, *B*). Therefore, the CD247 WT protein is normal in carriers of the p.Q101X mutation. We believe this may explain the observed discrepancies, as the relative proportions of the 2 isoforms may impact mAb binding both intracellularly and extracellularly in different moments of T-cell differentiation both *in vivo* and *in vitro*.

The immunologic workup had shown that T-cell maturation was essentially normal in mutation carriers (Table I) except for a slight increase of TEMRA and/or $CD45R0^+$ $CD4^+$ T cell subsets in several mutation carriers, either patients or relatives. Standard T-cell functional tests, such as proliferation after PHA-L or anti-CD3 stimulation, were also normal or even high (Table I; Fig E4 in the Online Repository available at www.jacionline.org). We therefore tested both early (CD69) and late (CD25) activation markers after CD3 and CD28 engagement (Fig E3 in the Online Repository available at www.jacionline.org). The results showed that the induction of CD69 was normal in all tested individuals and studied T-cell subsets. However, we noted low induction of CD25 in 4 of 5 tested mutation carriers for $CD8^+$, but not $CD4^+$, T cells. Together, these results suggested that despite the observed CD3 and CD247 expression defects, strong functional defects were not observed in T cells of mutation carriers, either patients or relatives. Subtle signaling dysfunctions with incomplete clinical penetrance, if present, could not be fully revealed using such standard functional tests.

We therefore went on to generate *in vitro* models where we could test the biochemical and functional features of the CD247 variants in monoclonal T-cell lines in the presence or absence of autologous WT CD247.

CRISPR/Cas9-edited CD247-deficient Jurkat T cells (ZKO) as a model system to test *CD247* nonsense variants *in vitro*

We next wanted to evaluate the potential impact of CD247 variants in TCR expression and function *in vitro*. This was done by testing them in 2 different scenarios: isolated in a CD247-deficient background (to test their potential to assemble a TCR/CD3 complex) or together with WT CD247 in a CD247-sufficient background such as Jurkat T cells, to test for potential dominant effects which might be relevant to our patients. To that end, CD247-deficient Jurkat T cells were generated using CRISPR/Cas9, which will be referred to as ZKO (Fig 4). Upon analysis by flow cytometry (using 6B10.2 mAb) and Western blot (using 6B10.2 and polyclonal antibody 448), we showed that ZKO cells lacked iCD247 (Fig 4, *A* and *B*). Moreover, these cells showed a marked reduction in extracellular CD3 expression (Fig 4, *C*), which was reversible upon lentiviral transduction of WT CD247 (Fig 4, *D*).

Nonsense, but not null, mutations ablating CD247 ITAMs were defective for normal TCR assembly and signaling and exerted a dominant-negative effect in normal TCR expression and signaling *in vitro*

Our patients showed CD247 variants that affected either 1 (Y152X) or 2 (Q101X) distal ITAMs in *CD247* Iso-1 and WT or in Iso-1 only, respectively. A range of CD247 nonsense variants have been reported previously (Fig 1, *B* and *C*), including Q142X and

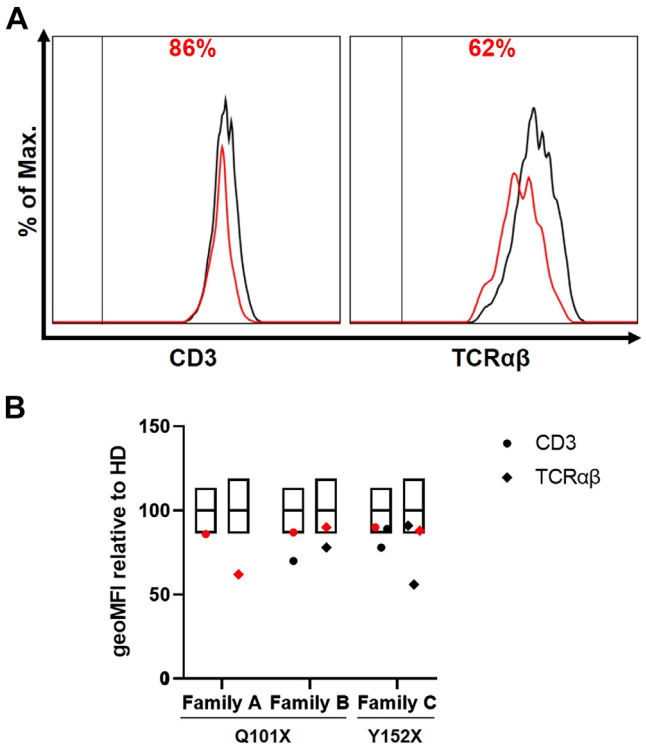

FIG 2. TCR αβ (IP26) and CD3 (UCHT-1) extracellular expression in $CD4^+$ cells. **(A)** Representative comparative histograms of patient AII.3 *(red histogram)* at 6 months of age vs a healthy donor *(black histogram)*. Values are % mean fluorescence intensity expression relative to the healthy donor. *Vertical line* represents the isotype control. **(B)** CD3 or TCR αβ expression levels in carriers from the indicated families in Table I normalized to healthy donor values (shown as mean and ranges). Index cases are represented in *red*. *geoMFI,* Geometric mean fluorescence intensity; *HD,* healthy donor; *Max.,* maximum.

Q70X, which ablated 1 and 3 distal ITAMs of both isoforms, respectively. We thus built plasmids carrying either WT/Iso-2 or Iso-1 splicing variants of normal CD247 as well as CD247 variants ablating 1 (Q142X), 2 (Q101X), or 3 (Q70X) ITAMs. These constructions were expressed by lentiviral transduction in a CD247-deficient background (ZKO) to test their potential to assemble a TCR/CD3 complex or in a CD247-sufficient background (Jurkat) to test for potential dominant effects. MOCK transduction served to test for null mutations that completely ablate CD247 expression.

The results in a CD247-deficient background showed that transduction of each of the 3 mutations into ZKO T cells could not restore normal surface TCR expression (60%, 22%, and 10% compared with WT, respectively) (Fig 5, *A*, bottom, and *B*). Interestingly, Iso-1 was also a weak isoform in terms of surface TCR expression restoration in ZKO (40% compared with WT). However, Q101X was still weaker (around 50% vs Iso-1). Together, these results showed that variant CD247 homodimers lacking any ITAMs due to nonsense mutations are defective for normal TCR assembly when CD247 was absent in an ITAM number-dependent fashion.

These results were further confirmed in a new set of experiments in which ZKO cells were transfected with the different CD247 variants linked to enhanced green fluorescent protein and then analyzed by flow cytometry and fluorescence microscopy (Fig E5 in the Online Repository available at www.jacionline.org). The flow cytometry results nicely reproduced those of Fig 5, *B* (compare with Fig E5, *B*), and the microscopy pictures revealed a differential distribution of enhanced green fluorescent protein fluorescence: Mock and Q70X mostly diffuse versus other variants, which are closer to membrane sites (Fig E5, *A*).

Lastly, to further support our findings, we made AlphaFold predictions of the 3D structure models of the studied variants. The results demonstrated that all CD247 variants have an impact on the 3D structure of the protein, even Iso-1, compared with WT. Moreover, the estimation of their folding free energy $\Delta G(T)$ showed that all variants are predicted to be more stable (ie, show lower folding free energy) than their corresponding normal isoform (Fig E6 in the Online Repository available at www.jacionline.org).

In a CD247-sufficient background, transduction of each of the 3 mutations (p.Q142X, p.Q101X, or p.Q70X) into Jurkat T cells reduced normal surface TCR expression (39%, 19%, and 9%, respectively, compared with WT) (Fig 5, *A*, top, and *C*). Note that WT transduction increased surface TCR expression compared with MOCK-transduced cells. Again, Iso-1 was weaker than WT in terms of surface TCR expression increase in Jurkat T cells (80% compared with WT). Together, these results showed that variant CD247 homodimers lacking any ITAM due to nonsense mutations reduced surface TCR expression when WT CD247 is present in an ITAM number–dependent fashion. In both systems, Iso-1 is a weak isoform compared with WT in terms of surface TCR expression.

To evaluate the potential impact of nonsense versus null *CD247* mutations in TCR function, we analyzed CD69 induction in all the T-cell lines in response to SEE-loaded Raji cells. The results showed that all cell lines carrying nonsense mutations were functionally impaired in this assay (25% to 50%) compared with the cell lines transduced with WT CD247, both in the presence of normal CD247 in WT Jurkat cells (Fig 6, *A*) or isolated in ZKO cells (Fig 6, *B*). These results suggested that nonsense *CD247* mutations were signaling deficient due to a dominant-negative effect in Jurkat T cells and could not signal downstream normally.

DISCUSSION

Our results in WT and ZKO Jurkat T cells suggest that variant CD247 homodimers lacking any ITAMs due to nonsense, but not null, mutations are defective for normal TCR assembly and exert a dominant-negative effect in normal TCR expression and signaling *in vitro*, which, in turn, may be associated with immunodeficiency or autoimmunity features *in vivo*, as observed in the studied index patients.

The variant-induced TCR expression defects occurred in a clear ITAM number–dependent fashion *in vitro* (Fig 5; Fig E7, *C*, in the Online Repository available at www.jacionline.org). A potential explanation for such differences may lie in the basic residue-rich stretches carried by each ITAM, which regulate the transport and surface expression of the TCR complex.[17] Nonsense mutations that remove a growing number of such stretches can thus increasingly affect TCR expression, as we have shown (Fig E5). Also, the predicted 3D structure models showed that all variants significantly change the structure of the CD247 WT isoform (Fig E6), which, in turn, may have an impact on TCR assembly and/or signaling.

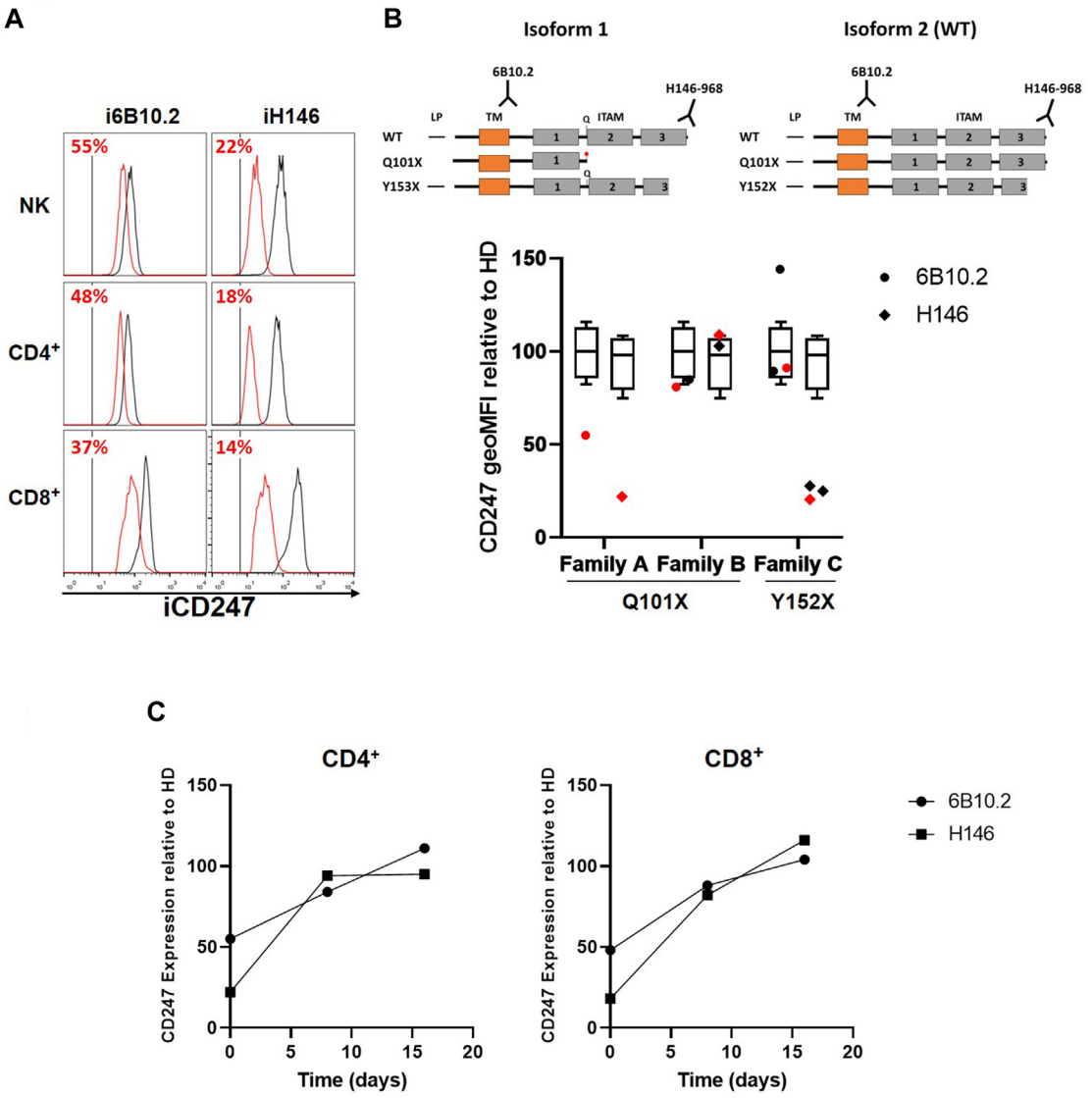

FIG 3. Expression of iCD247 in primary cells. Flow cytometry analysis of iCD247 using 6B10.2 and H146-968 mAbs in $CD4^+$, $CD8^+$, and NK lymphocytes in the indicated individuals. **(A)** Comparative histograms of iCD247 expression in patient A II.3 *(red histogram)* at 6 months old vs a healthy donor *(black histogram)* in $CD4^+$, $CD8^+$, and NK cells. Values represent expression % relative to healthy donors. *Vertical line* indicates the isotype control. **(B)** Schematic representation of the impact on CD247 of the mutations studied in both isoforms and how they affect the recognition of the anti-CD247 antibodies used in $CD4^+$ cells. iCD247 expression in $CD4^+$ cells in the studied families normalized to healthy donor values (shown as mean and ranges) at the age shown in Table I. Index cases are represented in *red*. **(C)** The iCD247 defect tends to disappear gradually over time. Flow cytometry analysis of iCD247 expression with the 6B10.2 and H146-968 antibodies in allogeneic feeder cultures of patient AII.3 at different times. Values show iCD247 expression relative to healthy donor culture. *H146,* H146-968; *HD,* Healthy donor.

By contrast, the variant-induced TCR signaling defects were not ITAM number dependent, but rather very similar (Fig 6). This fits with reports showing that the importance of each ITAM domain is not only quantitative in mice.[3] Rather, the sequence of each ITAM is crucial for thymic development, with the third ITAM of CD247 being the most critical compared with the rest. Indeed, Q142X ablates the third CD247 ITAM, as is also the case for Q101X and Q70X, which may explain their similar functional impact.

Interestingly, we find a sharp contradiction between predicted combined annotation-dependent depletion mutation pathogenicity values (Fig 1, *C*) and surface TCR expression in ZKO T cells (Fig 5, *B*) or number of active ITAMs (Fig 1, *B*) for the CD247 mutations tested in this work (Fig E7). According to our cellular ZKO model, surface TCR expression increased with the number of ITAMs (Fig E7, *C*), whereas predicted pathogenicity unexpectedly increased with TCR expression or the number of ITAMs (Fig E7, *A* and B). We believe that our phenotypical and functional results hold true better than combined annotation-dependent depletion estimations. Indeed, Q70X is known to be absent from the population and extremely severe clinically (Fig 1,*C*) (see also Rieux-Laucat et al[18]), whereas Q142X and Q101X are quite frequent (Fig 1, *C*) but have not been reported to cause immunopathology to date.

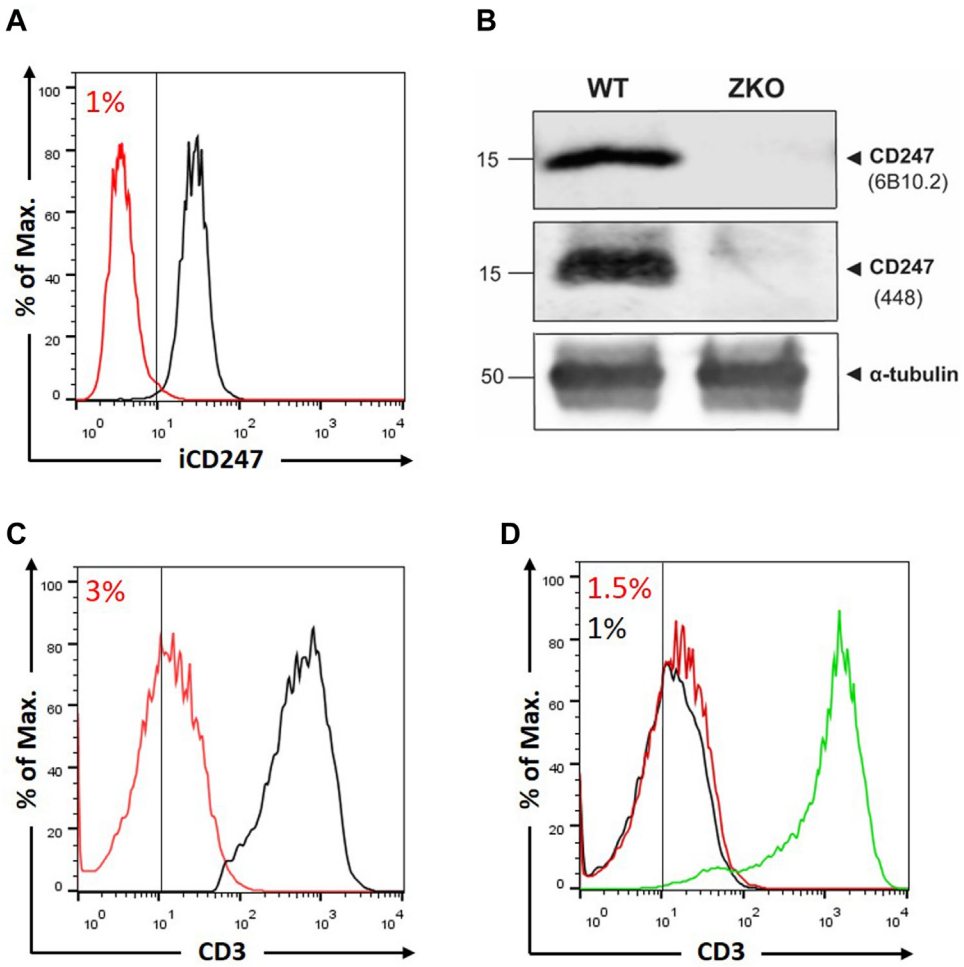

FIG 4. Jurkat *CD247*$^{-/-}$ (ZKO) cell line validation. **(A)** iCD247 in WT Jurkat cells *(black)* and the ZKO line *(red)*. Vertical line represents the isotype control. **(B)** Western blot analysis of whole lysates of cells from *(A)* using the indicated iCD247-specific antibodies, with α-tubulin as loading control. **(C)** Extracellular expression of CD3 in cells from *(A)*. *Vertical line* represents the isotype control. **(D)** Reconstitution of CD3 expression in ZKO line *(red)* after lentiviral transduction with empty viral vector (MOCK) *(black)* and WT CD247 *(green)*. Values indicate the percentage of expression relative to the parental line. *Max.,* maximum.

These counterintuitive findings may be relevant in the context of chimeric antigen receptor T-cell design, as shown recently in mice.[5]

The surface TCR expression defects found *in vitro* in Jurkat T-cell models in the presence or absence of autologous WT CD247 transduced with the different truncated *CD247* variants tested in this work were stronger than those found in primary T cells of truncated variants carriers *ex vivo* (compare Figs 2 and 5). Similarly, strong functional defects were not observed in mutation carriers, either patients or healthy relatives, indicating that we are dealing with subtle dysfunctions with incomplete clinical penetrance (only 4 of the 6 mutation carriers had immune pathology features) that cannot be revealed using standard functional tests. We believe this may be due to thymic selection pressures on polyclonal T-cell repertoires that are not present in Jurkat T cells. Indeed, some indication of abnormal T-cell selection or function may be appreciated *ex vivo* in tested mutation carriers, both patients and relatives, with incomplete penetrance: (1) increased TEMRA and/or CD45R0^{+} memory CD4^{+} T-cell subsets in 3 of 5, as noted in congenital immunodeficiencies of the TCR[19,20]; (2) low TCR-mediated induction of CD25 in CD8^{+} T cells in 4 of 5; and (3) autoimmune features in 3 of 6. Reduced expression of CD247 is considered a biomarker in several autoimmune diseases such as lupus, systemic sclerosis, or rheumatoid arthritis.[21] Similarly, *CD247* polymorphisms have been reported to correlate with the presence of rheumatoid factor autoantibodies.[22] Also, by using a mutant mouse line expressing a hypomorphic allele of CD247, the strength of pre-TCR–mediated signaling during T-cell development was shown to determine the diversity of the TCR β repertoire available for positive and negative selection and hence of the final TCR αβ repertoire.[23]

Similar subtle dysfunctions may have an impact in autoimmunity or immunodeficiency features in *CD247* mutation carriers, as we have observed. The Q101X warrants further discussion. A factor that may be relevant in Q101X is age and Iso-1 versus Iso-2 (WT) splicing regulation: whereas in family C (Y152X mutation), differences in CD247 expression were not observed between the pediatric subjects and the mother, in the Q101X mutation, a considerable difference was observed between patient AII.1 and the adult subjects of family B (Fig 3, *B*). The difference

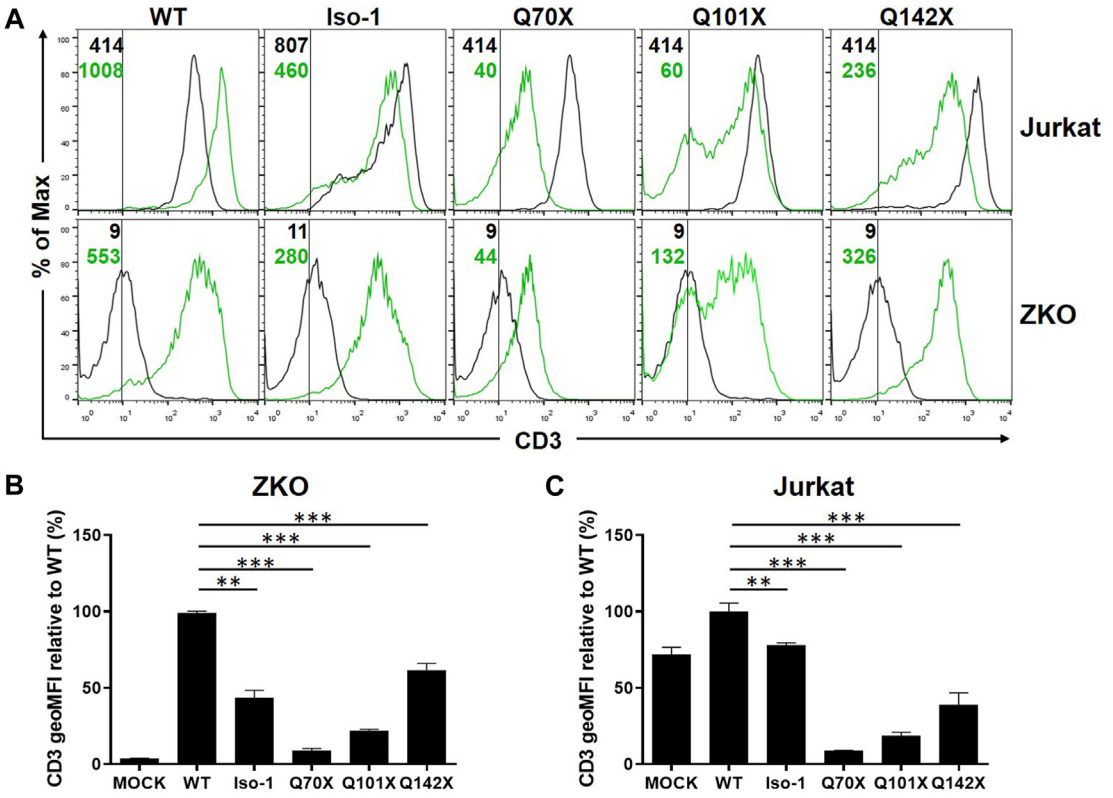

FIG 5. Extracellular CD3 expression **(A)** in Jurkat and ZKO cells transduced with the different CD247 variants *(green histogram)* vs MOCK *(black histogram)*. Numbers in each color indicate the mean fluorescence intensity of that experiment. *Vertical line* represents the upper limit of the isotype control. Quantification of *(A)* in ZKO **(B)** and Jurkat **(C)** cells. n = 4. $^{**}P < .01$, $^{***}P < .001$. *geoMFI,* Geometric mean fluorescence intensity.

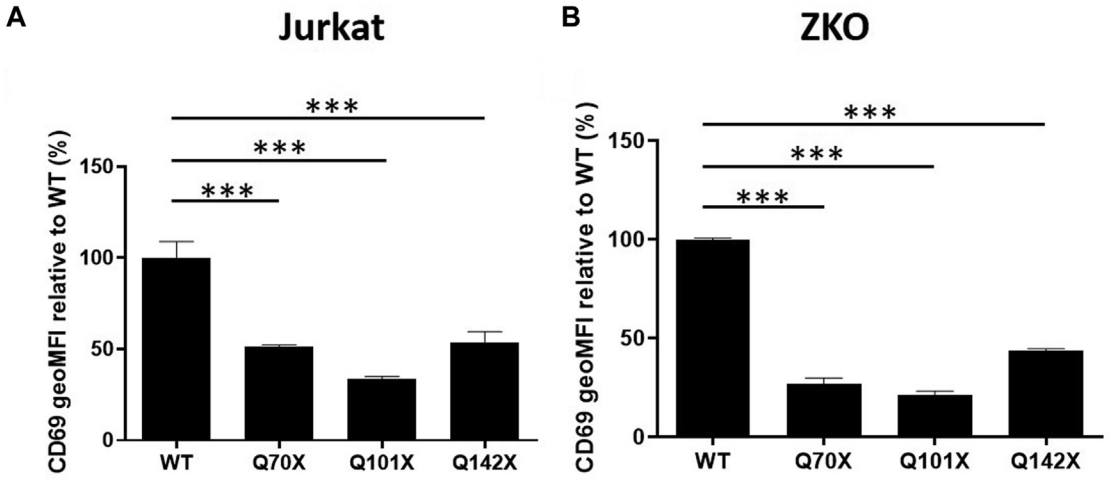

FIG 6. CD69 induction after TCR stimulation for 24 hours in Jurkat-Raji/SEE **(A)** or ZKO-Raji/SEE conjugates **(B)** transduced with different CD247 constructs. n = 3. $^{***}P < .001$. *geoMFI,* Geometric mean fluorescence intensity.

can emerge from the peculiar Q101X mutation, which affects only the minor Iso-1, and over time it can select lymphocytes with higher expression of unmutated Iso-1 from the normal chromosome. Such selective pressures for more functional CD247 have been clearly demonstrated for CD247 revertant T, but not NK, cells in CD247-deficient patients.[19] The data from allogeneic cultures showing the selection of T cells with high levels of CD247 would corroborate the hypothesis, although it was not possible to verify which isoforms were expressed due to lack of sample availability (Fig 3, *C*). Unmutated CD247 splicing Iso-1 was a poor partner for surface TCR expression when isolated or accompanied by Iso-2/WT (Fig 5), suggesting that regulation of

Iso-1 levels may impact T-cell function. Mutation Q101X strongly increased these inhibitory properties, including in TCR function (Fig 6). It has been observed that Iso-1 has remained unchanged since the separation of primates and ungulates in the Cretaceous period around 80 to 100 million years ago.[16] It is very likely that this degree of conservation must have some significant functional implications. It has been proposed that splicing variant Iso-1 may be inhibitory during T-cell activation. The upregulation of the relative proportion of Iso-1 transcripts during prolonged T-cell activation probably raises the number of receptors needed to achieve an activation threshold.

Last, although the information obtained from primary T cells from mutation carriers is scarce due to limited sample accessibility, we believe, as reported,[24] that even rare findings in experiments of nature may be relevant in the field. Modeling the variants *in vitro* in appropriate T-cell systems, as we have done, may reveal aspects that are difficult to prove in primary cells.

Note added in proof: A fourth unrelated patient carrying the p.Q101X mutation was characterized and treated from 9 years of age with signs of immunodeficiency including recurrent perioral herpes simplex virus susceptibility complicated by meticillin-sensitive *Staphylococcus aureus* bacterial superinfection, recurrent otitis, T, B, and NK lymphopenia, and low Ig levels. All normalized by age 16.

DISCLOSURE STATEMENT

This work was supported by grants from the Ministerio de Economía y Competitividad (MINECO PID2021-125501OB-I00 and RTI2018-095673-B-I00) and Asociación Española Contra el Cáncer (AECC PROYE20084REGU). A.C.B. was supported by Complutense University scholarship (CT27/16 and CT31/21). R.F.M. and D.C.A. were supported by the Spanish Ministry of Science, Innovation and Universities (FPU19/03136 and PRE2019-088150). P.P.C. was supported by Juan de la Cierva-Incorporación fellowship (IJCI-2014-19262).

Disclosure of potential conflict of interest: The authors declare that they have no conflicts of interest.

Key messages

- **Heterozygous nonsense mutations that truncate ITAMs were identified in 3 patients exhibiting signs of immunodeficiency or autoimmunity.**
- ***In vitro* studies showed that truncated CD247 variants impaired proper TCR assembly and signaling in a manner dependent on the number of missing ITAMs.**
- **This dominant-negative effect in T cells may correlate with clinical features observed *in vivo*.**

REFERENCES

1. Alcover A, Alarcón B, Di Bartolo V. Cell Biology of T cell receptor expression and regulation. Annu Rev Immunol 2018;36:103-25.
2. Call ME, Pyrdol J, Wiedmann M, Wucherpfennig KW. The organizing principle in the formation of the T cell receptor-CD3 complex. Cell 2002;111:967-79.
3. Bettini ML, Chou PC, Guy CS, Lee T, Vignali KM, Vignali DAA. Cutting edge: CD3 ITAM diversity is required for optimal TCR signaling and thymocyte development. J Immunol 2017;199:1555-60.
4. Feucht J, Sun J, Eyquem J, Ho YJ, Zhao Z, Leibold J, et al. Calibration of CAR activation potential directs alternative T cell fates and therapeutic potency. Nat Med 2019;25:82-8.
5. Gaud G, Achar S, Bourassa FXP, Davies J, Hatzihristidis T, Choi S, et al. CD3ζ ITAMs enable ligand discrimination and antagonism by inhibiting TCR signaling in response to low-affinity peptides. Nat Immunol 2023;24:2121-34.
6. Geisler C, Kuhlmann J, Plesner T, Rubin B. Failure to synthesize the human T-cell CD3-ζ chain and its consequence for the T-cell receptor-CD3 complex expression. Scand J Immunol 1989;30:191-7.
7. Marin AVM, Garcillán B, Jiménez-Reinoso A, Muñoz-Ruiz M, Briones AC, Fernández-Malavé E, et al. Human congenital T-cell receptor disorders. LymphoSign Journal 2015;2:3-19.
8. Jumper J, Evans R, Pritzel A, Green T, Figurnov M, Ronneberger O, et al. Highly accurate protein structure prediction with AlphaFold. Nature 2021;596:583-9.
9. Hiranuma N, Park H, Baek M, Anishchenko I, Dauparas J, Baker D. Improved protein structure refinement guided by deep learning based accuracy estimation. Nat Commun 2021;12:1340.
10. Echols N, Grosse-Kunstleve RW, Afonine PV, Bunkóczi G, Chen VB, Headd JJ, et al. Graphical tools for macromolecular crystallography in *PHENIX*. J Appl Crystallogr 2012;45:581-6.
11. Pucci F, Kwasigroch JM, Rooman M. SCooP: an accurate and fast predictor of protein stability curves as a function of temperature. Bioinformatics 2017;33:3415-22.
12. Zhang P, Bigio B, Rapaport F, Zhang SY, Casanova JL, Abel L, et al. PopViz: a webserver for visualizing minor allele frequencies and damage prediction scores of human genetic variations. Bioinformatics 2018;34:4307-9.
13. Apoil PA, Puissant-Lubrano B, Congy-Jolivet N, Peres M, Tkaczuk J, Roubinet F, et al. Reference values for T, B and NK human lymphocyte subpopulations in adults. Data Brief 2017;12:400-4.
14. Schatorjé EJH, Gemen EFA, Driessen GJA, Leuvenink J, van Hout RWNM, de Vries E. Paediatric reference values for the peripheral T cell compartment. Scand J Immunol 2012;75:436-44.
15. Tosato F, Bucciol G, Pantano G, Putti MC, Sanzari MC, Basso G, et al. Lymphocytes subsets reference values in childhood. Cytometry A 2015;87:81-5.
16. Atkinson TP, Hall CG, Goldsmith J, Kirkham PM. Splice variant in TCRζ links T cell receptor signaling to a G-protein-related signaling pathway. Biochem Biophys Res Commun 2003;310:761-6.
17. DeFord-Watts LM, Dougall DS, Belkaya S, Johnson BA, Eitson JL, Roybal KT, et al. The CD3 ζ subunit contains a phosphoinositide-binding motif that is required for the stable accumulation of TCR-CD3 complex at the immunological synapse. J Immunol 2011;186:6839-47.
18. Rieux-Laucat F, Hivroz C, Lim A, Mateo V, Pellier I, Selz F, et al. Inherited and somatic *CD3* ζ mutations in a patient with T-cell deficiency. N Engl J Med 2006;354:1913-21.
19. Marin AV, Jiménez-Reinoso A, Briones AC, Muñoz-Ruiz M, Aydogmus C, Pasick LJ, et al. Primary T-cell immunodeficiency with functional revertant somatic mosaicism in CD247. J Allergy Clin Immunol 2017;139:347-9.e8.
20. Rowe JH, Delmonte OM, Keles S, Stadinski BD, Dobbs AK, Henderson LA, et al. Patients with CD3G mutations reveal a role for human CD3γ in Treg diversity and suppressive function. Blood 2018;131:2335-44.
21. Dexiu C, Xianying L, Yingchun H, Jiafu L. Advances in CD247. Scand J Immunol 2022;96:e13170.
22. Li P, Wang X, Zhao MQ, Li LJ, Zhang C, Li BZ, et al. TCR-CD3ζ gene polymorphisms and expression profile in rheumatoid arthritis. Autoimmunity 2016;49:466-71.
23. Bovolenta ER, García-Cuesta EM, Horndler L, Ponomarenko J, Schamel WW, Mellado M, et al. A set point in the selection of the αβTCR T cell repertoire imposed by pre-TCR signaling strength. Proc Nal Acad Sci 2022;119:e2201907119.
24. Casanova JL, Conley ME, Seligman SJ, Abel L, Notarangelo LD. Guidelines for genetic studies in single patients: lessons from primary immunodeficiencies. J Exp Med 2014;211:2137-49.